

Assessing the impact of WEC arrays on the nearshore wave climate and power production on the Dutch coast

Wells, Sarah; Alday, Matias; Ilzarbe, Jesús Maria Blanco; Lavidas, George

10.1016/j.energy.2025.136698

Publication date

Document Version Final published version

Published in Energy

Citation (APA)

Wells, S., Alday, M., Ilzarbe, J. M. B., & Lavidas, G. (2025). Assessing the impact of WEC arrays on the nearshore wave climate and power production on the Dutch coast. *Energy*, *331*, Article 136698. https://doi.org/10.1016/j.energy.2025.136698

Important note

To cite this publication, please use the final published version (if applicable). Please check the document version above.

Copyright

Other than for strictly personal use, it is not permitted to download, forward or distribute the text or part of it, without the consent of the author(s) and/or copyright holder(s), unless the work is under an open content license such as Creative Commons.

Please contact us and provide details if you believe this document breaches copyrights. We will remove access to the work immediately and investigate your claim.



Contents lists available at ScienceDirect

Energy

journal homepage: www.elsevier.com/locate/energy





Assessing the impact of WEC arrays on the nearshore wave climate and power production on the Dutch coast

Sarah Wells a,*, Matías Alday b, Jesús Maria Blanco Ilzarbe b, George Lavidas b

- ^a School of Engineering, Universidad del País Vasco/Euskal Herriko Unibertsitatea, Bilbao, Spain
- b Marine Renewable Energies Lab, Offshore Engineering Section, Department of Hydraulic Engineering, Civil Engineering & Geo-sciences, Delft University of Technology, Delft, Netherlands

ARTICLE INFO

Keywords: SWAN Wave energy array Resource assessment Capacity factor Netherlands

ABSTRACT

As the necessity for the decarbonisation of the global electricity market increases, a range of renewable energy technologies will be implemented, one of which is wave energy. A key step in this process is the thorough quantification of both the power resource at locations of interest, and the impacts of these devices on the natural environment. The present work streamlines these 2 processes into one methodology by investigating the long-term impacts of an array of 20 WECs on the nearshore Dutch wave climate, while also calculating the potential power resource at the site considering intra-array wake effects. Simulations of 10 year duration were conducted in the baseline scenario (no farm present) and with 2 array configurations, using the spectral wave model SWAN on an unstructured mesh. It was demonstrated that the power production of the farm during this period, when wake effects are considered, is calculated to be up to 1.8% less than traditional methods. The presence of the farm is shown to reduce significant wave height and wave power in its lee, with the effects being largely attenuated at the coast. It was shown that the magnitude of the change is dependent on both the period and height of the waves at the farm, and notably the magnitude of the reduction does not increase consistently with the wave height, contradicting the sentiment that wave farms are effective protection mechanisms against damaging high-energy conditions. Furthermore, the present work suggests that changes to the nearshore breaker index may impact longshore currents that are essential for nutrient and sediment transport, the effect of which on the ecosystem is not yet well quantified.

1. Introduction

Within the European Union (EU), the electricity sector is currently responsible for more than 25% of greenhouse gas emissions [1]. The anthropogenic contribution of Climate Change has been closely documented [2], and the need to decarbonise the global energy mix has increased in recent decades. In light of this, the EU has gradually implemented increasingly ambitious targets to allow Europe to become the first carbon-neutral continent by 2050 [3]. In order to achieve this target, all 27 EU member states have pledged to reduce emissions by 55% by 2030 compared to 1990 levels [3]. A key step required to achieve this is the rapid implementation of renewable energy which will assist in the decarbonisation of not only the electricity sector, but also the transport sector as vehicles are increasingly electrified. To assist the increasing penetration of renewables into the electricity mix and to satisfy current targets, a range of technologies are predicted by the International Energy Agency to play key roles [4]. Utilisation of wave energy is one such resource that has attracted attention as a viable solution to contribute to renewable energy penetration in the EU. In fact, current targets stated by the European Commission aim to reduce the cost of wave energy to €0.20 per kWh by 2025 and €0.15 per kWh by 2030, aiming at capacity of ocean energies in EU at least 40GW by 2050 [5]. The distribution of this deployment will, like all offshore technologies, be heavily concentrated in coastal countries. In the case of wave energy, the potential resource is concentrated on the Atlantic coast of Europe [6]. In the Netherlands, a country with most population centres and demand along the coast, it has been proposed that a WEC installed capacity of up to 24 MW by 2030 and 44 MW by 2040 should be aimed for [7]. However, for the implementation of wave energy converters to be viable, their projected power output and environmental impacts both positive and negative must be well quantified.

There are several papers currently in the literature that describe the potential effects of WEC arrays on the wave field present at the

E-mail address: swells001@ikasle.ehu.eus (S. Wells).

^{*} Corresponding author.

coast. The existing literature regarding spectral simulations investigates the influence of several key parameters; coast-farm distance, WEC array configuration and alongshore position. A range of studies have been conducted using wave averaged spectral models to estimate the short-medium term effects of WEC arrays on the nearshore wave climate.

These studies emphasise that the placement of wave farms can significantly affect the coastal impacts, although not always in a predictable way. It was shown [8] that increasing the farm-coast distance may not always decrease the maximum nearshore impact, but that it will alter the position of this point. In Rodriguez et al. 2018 [9], the alongshore position was shown to be extremely important with regards to morphological effects, as the relative placement of the farm may change effects from erosionary to accretionary. This effect is highly site-dependent, and must therefore be closely investigated on a case-by-case basis before potential farms are implemented. It was asserted in [10] that the effects of WEC arrays can increase with decreasing farm-coast distance, and that this effect is most pronounced in sea states with minimal directional spreading.

The relative impact of farms placed in single- or two-row arrays has been investigated in [11], showing that array configuration is most relevant at sites close to shore and has negligible impact at large distances (>5 km) from the shore at the zone examined. The dependency of spacing and arrangement of WECs in a farm on the morphological impact has been examined [12,13], showing that the beach profile can be highly sensitive to small changes.

Despite the existence of these studies in the literature, they all suffer from short term duration (\sim 1 year) [14,15], which cannot satisfy the criteria for the minimum duration of a resource assessment for 10 years [16].

However, WEC farms' predominant function is to produce renewable electricity. Evaluating the power-producing capabilities of WEC devices in a particular region requires 2 key pieces of information: the wave climate at the site of interest, and the interaction of the device with the wave field. In order to quantify this interaction, a WEC device has an associated power matrix that quantifies the amount of power produced in particular wave conditions, described by H_s and T_p . Estimations of the energy producing capabilities of a WEC at a particular site are frequently made by using this matrix with a time-series dataset of wave parameters [17-19]. This method does not accurately represent the potential impacts that intra-array wake effects may have on the total energy production. This method can be improved upon by determining the q-factor of an array in one or more sea states. The q-factor is defined as the ratio of energy absorption by a device in an array to a device in isolation. By defining this parameter using static simulations in many sea states that describe a particular wave climate [20], the overall energy absorption of the array can be estimated. This methodology, however, requires the running of simulations that encompass all possible sea states.

To complement the existing literature, this study focuses on a region in the north of the Netherlands, as a case study, and investigates both the power production and coastal wake effects that WEC arrays will have. The region selected is in accordance with past research [21], and aims to enhance existing literature by revealing the long-term coastal impacts while considering intra-array effects on power production. In accordance with the shallow nature of the region selected, the WEC device to be studied is based on the Oyster WEC, an oscillating-wavesurge-converter [OWSC] device that is designed to absorb energy in water depths of 10-15 m. While previous studies, as discussed above, have touched upon the role of farm configuration on nearshore processes in the short-term, most have been applied for only singular sea states (with particular focus on damaging storm conditions), with some conducting up to 1 week of simulation [22]. Furthermore, none of the aforementioned studies have looked into the impacts of the capacity factors of individual WECs within an array during a simulation conducted for the purpose of resource evaluations.

Our study looks into the impacts of OWSC-type WEC arrays on the wave climate and quantitatively assesses the potential array impacts in power production, considering a decadal range of metocean parameters. Uniquely, this analysis considers the long-term (≥10 years) and also looks into the seasonal (winter–summer) effects that the WEC arrays are expected to have. The study underlines the pitfalls of assessing power performance of arrays without considering their array interactions, leading to over-estimations of their produced power.

2. Materials & methods

The study area of our model lies just outside the Wadden Sea, which has been flagged as one of the most interesting in the Netherlands [21] , whilst also having a high impact by coastal erosion. A wave spectral phase average model, the Simulating WAves Nearshore is utilised to produce long-term information with and without the presence of the array. In order to retrieve long-term results describing the everchanging conditions of the sea, a non-stationary model is implemented. The duration of the model is from 2011-2020, and utilises spectral boundary conditions provided by the ECHOWAVE database [23,24] provided by the Marine Renewable Energies Lab (MREL) at TU Delft at hourly resolution. The ECHOWAVE dataset provides the wave spectrum relative to both wave frequency and direction in European Atlantic waters at hourly resolution. As the spectral boundary conditions (obtained using Wavewatch III in [24]) are applied directly into the model, no assumptions regarding the spectral shape are imposed on these inputs. These spectral boundary conditions, along with wind inputs applied throughout the domain obtained from the ERA5 dataset [25], allow the SWAN model to calculate the evolution of the spectral action balance equation without any a priori restrictions on the spectrum [26]. The spectral data from three distinct grid points of the ECHOWAVE hindcast dataset are implemented to apply boundary conditions on each of the three sea boundaries of the model domain shown in Fig. 1. The nearest available points are selected for each boundary.

The SWAN model is then implemented in the third generation mode using the ST6 formulation with HWANG and DEBIAS formulations dictating the influence of wind on the spectral evolution, with a wind drag coefficient of 35. Influences on the spectra from quadruple interactions (fully explicit formulation), wave breaking, friction (JONSWAP constant 0.038), triad interactions and diffraction are also considered. These physics parameters are obtained from [27], based on a thorough convergence study conducted in the North Sea. These parameters were shown to most accurately describe the wave climate in this region, after a rigorous calibration and validation process.

Unlike other resource assessments, our focus is to evaluate the effects of WEC arrays, hence a high fidelity mesh is needed for both the resolving the surrounding topobathymetry and for the modelling of the wave-structure interactions. To satisfy these requirements an unstructured mesh is implemented, allowing high refinements in areas of interest while maintaining coarse resolution in deep water. In order to achieve this, the Matlab package OceanMesh2D [28] is utilised.

The refinement of the mesh near the shore is a compromise between several factors. While finer resolution can better resolve geographical and bathymetric features, it will result in a higher number of elements and a higher computational time. Furthermore, too fine of a mesh can result in the Courant–Friedrichs–Lewy [CFL] condition being significantly violated. Although this criterion is not demanded by SWAN due to the stability of the implicit scheme used, if this condition is too heavily exceeded it can violate causality and produce non-physical results. For this study, an unstructured mesh that has a resolution of 100 m nearshore is implemented in order to resolve the necessary coastal features without producing physical instabilities.

For the wave farm to be implemented in SWAN, the resolution of the mesh surrounding the farm must be sufficiently high that the features may be resolved. Technically, this requires that the maximum mesh size in this region must be smaller than the size of the WEC object. In

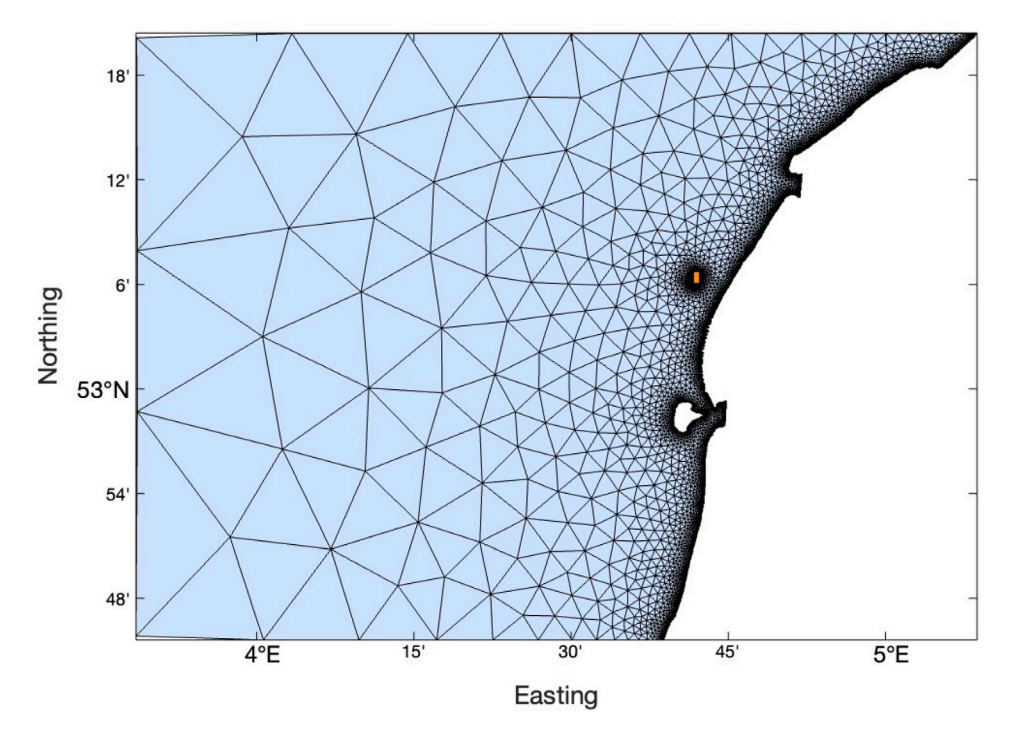


Fig. 1. Unstructured mesh generated by OceanMesh2D [28]. Approximate farm location is shown in orange. (For interpretation of the references to color in this figure legend, the reader is referred to the web version of this article.)

this case, the resolution in the farm region is defined to be between 10–15 m. As discussed previously, refinement of this magnitude may produce some physical instabilities in the event that waves have a large group velocity compared with the timestep of the simulation. According to the dispersion relation, defined by

$$\lambda = \frac{gT^2}{2\pi} \tanh\left(\frac{2\pi d}{\lambda}\right),\tag{1}$$

waves with particularly long periods will have high phase and group velocities and may lead to unstable results.

However, given the requirements for resolving the WEC arrays effectively, this compromise must be made. An alternative solution would be to decrease the timestep implemented in the model, however as this work involves 10 years of simulation, this cannot be excessively minimised. There is therefore again a compromise between accuracy and computational expense. In these simulations, a timestep of 5 min is implemented.

Fig. 1 depicts the mesh implemented for these simulations. The final mesh used contains 26,389 line elements connecting 13,705 nodes.

Within SWAN, obstacles can be defined that act as wave 'blockers', limiting the transfer of the action potential between adjacent nodes if the obstacle crosses the connecting line. The extent to which the action potential is blocked is defined by the transmission coefficient C_t , defined by the ratio of wave heights immediately before and after the obstacle;

$$C_t = \frac{H_{leeward}}{H_{seaward}}. (2)$$

For the present work, the transmission coefficient was chosen to be 0.1, and the reflection coefficient was chosen to be 0.5. This indicates that 10% of the wave height is permeating through the device, and that 50% is reflected. These values were chosen so as to represent the physical properties of an almost impermeable 'wall', as a simple representation of an Oyster WEC. The authors acknowledge that this represents a simplification of the hydrodynamics associated with OWSC devices, which are not in fact semi-transparent walls, but interact dynamically with the incoming wave field. It remains an avenue for further research for the frequency- and directionally- dependent nature

of the wave-structure interaction to be implemented in this model. This methodology, however, provides useful indications regarding the behaviour of WEC arrays in long-term sea climates.

In order to conduct this investigation into the power-producing capabilities and the nearshore impacts of the WEC devices, three simulations of 10-year duration are run. The first, explored in Section 4.1, constitutes a baseline scenario, in which no WECs are implemented in the model. Using this result, the hypothetical power production of the device in this location using the conventional power matrix approach are calculated. The subsequent two simulations involve the implementation of WEC arrays (see Fig. 2) in the model with 3L and 5L intra-array spacing (where L is the length of the WEC). From these results, wave parameters from points immediately seaward of each device can be extracted and used with the WEC power matrix to calculate their energy yield individually. This approach, unlike that of the baseline scenario, considers the interaction of the wave field with the WEC arrays when determining power production.

3. Validation study

Although the physics of the model is based on a past publication [27], because a new ultra-high fidelity is used, this study undertakes a validation compared with an in-situ buoy to ensure that our new hindcast is not influenced by numerical instabilities.

For this reason, a SWAN hindcast was conducted using the generated mesh and model setup for the 3 year period from 2018–2020 with no wave farm present. These results were compared with the in situ data provided by the WaddenEierlandseGat metocean buoy provided by Rijkswaterstaat, the Dutch Ministry of Infrastructure and Water Management. For the years considered, the significant wave height was shown to satisfy statistical parameters as shown in Table 1. The correlation coefficient can be seen to be high for all years compared, demonstrating that the model is simulating the parameter well. The mean bias can be seen to vary between 18–29 cm in the 3 years, suggesting that the model overestimates the wave resource on average. The low scatter index demonstrates that the variability of the model data is consistent with the variability of the in-situ data.



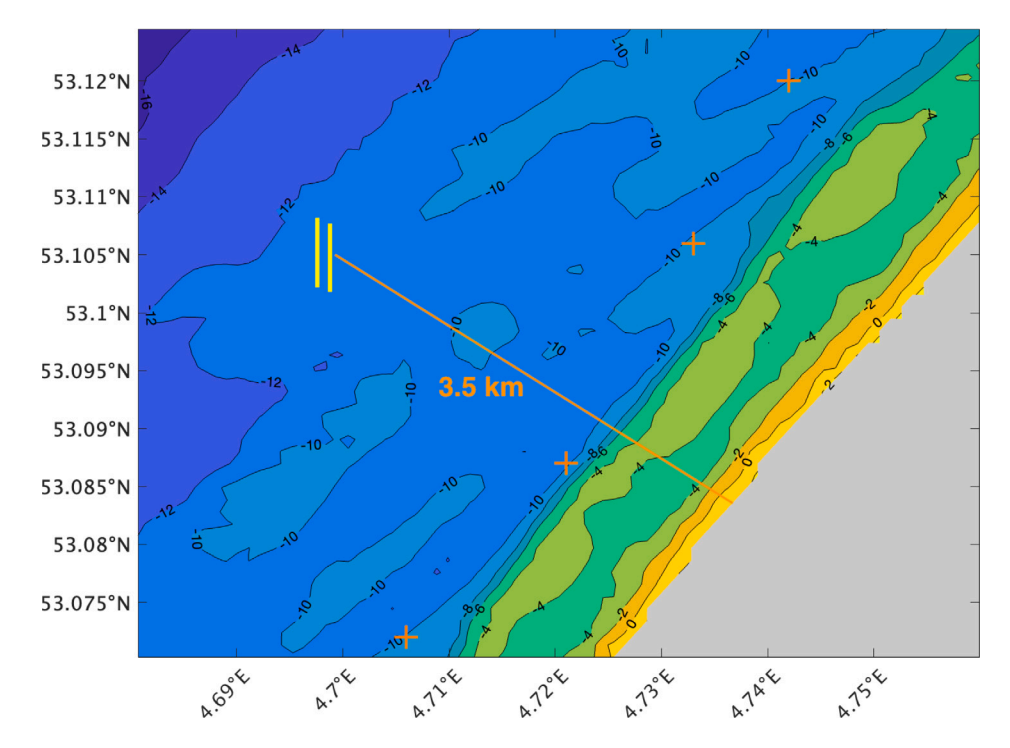


Fig. 2. Local bathymetry and WEC farm configuration. Crosses denote points at which additional analysis was conducted alone the 10 m contour.

Table 1 Statistical parameters comparing SWAN results for significant wave height H_s with in situ data.

R	MB [m]	SI	Number of Measurements
0.942	0.202	0.052	7777
0.940	0.187	0.063	4297
0.935	0.286	0.073	4637
	0.942 0.940	0.942 0.202 0.940 0.187	0.942 0.202 0.052 0.940 0.187 0.063

Table 2 Statistical parameters comparing SWAN results for peak period T_p with in situ data.

	R	MB [m]	SI	Number of Measurements
2018	0.706	-0.028	0.310	7777
2019	0.703	0.031	0.369	4297
2020	0.639	0.271	0.447	4631

For the peak period, the statistical parameters are shown below in Table 2. Although the correlation coefficient is lower for this parameter, this is related to the nature of the peak period and does not indicate that the model is not, in general, well-representing the wave climate. The mean bias for this parameter corroborates this, as it shows that the peak period is estimated very well on average. The scatter index is, again, greater for this parameter, which is related to the different discretisation of the buoy compared with the model.

4. Results

4.1. Baseline scenario

In the region the mean power flux exceeds 10 kW/m during the 10 year period, see Fig. 3. When seasonal effects are considered it can be seen that this energy is concentrated during the winter months, in which the power flux exceeds $18 \ kW/m$. In contrast, the summer resource has a mean value of approximately $6 \ kW/m$, see Fig. 4.

The values in the joint distribution diagram (see Fig. 5) represent the portion of time [in %] during which the wave climate is described by the relevant values of H_s and T_p , while the colours represent the associated yearly energy flux. It can be seen that the largest portion

of time is taken up by sea states in which $H_s=1.5~\mathrm{m}$ and $T_p=6~\mathrm{s}$. Despite these sea states being most common, the majority of the energy being produced occurs at sea states for which $H_s=3~\mathrm{m}$ and $T_p=8~\mathrm{s}$, at which an average of 3.2 MWh is available per year.

In these sea states, the Oyster WEC is rated to produce 241 kW. The sea states during which the Oyster is rated to produce maximum power, 290 kW, are those with H_s between 4–6 m and T_p from 7–8 s, or with H_s at 4–4.5 m and T_p at 6 s. Unfortunately, these sea states occur minimally at the site in question. Based on the wave resource examined, the hypothetical energy produced by a single Oyster device in each year simulated is shown in Table 3. The variability in the yearly energy production is approximately 200 MWh, with the maximum theoretical yield being 707 MWh in 2015 and the minimum being 510 MWh in 2018.

There are clear seasonal trends in the energy yield, with the winter being the most profitable and summer being generally the least, which is consistent with the predictions made based on the wave climate. The capacity factor of this WEC varies from 20%–28% throughout the simulated years, demonstrating the importance of conducting long-term simulations to accurately estimate the power producing potential of a WEC array. While emphasis is often placed on intra-annual variation of the wave resource with the seasons, there can also be strong inter-annual variation occurring due to larger scale climate events.

4.2. Power performance with WEC arrays included in simulation

Fig. 6 depicts the capacity factor calculated for each of the devices for each of the years simulated. It demonstrates very clearly that there is a significant difference in the amount of power captured by the WECs in the row closest to shore compared to the row closer to the open sea. While the power capture of the seaward row is relatively consistent for all devices, it can be seen that the power captured by the leeward row is significantly less.

The effect of this is concentrated in the centre of the row. This result confirms that the capacity factors of the array devices calculated using the conventional methods will be an overestimation. Comparing the results obtained for the 3L and 5L array configurations, the magnitude of the capacity factors in each case appear to be similar. However,

 $\textbf{Table 3}\\ \textbf{Hypothetical energy produced per device per year from 2011-2020, without intra-array effects considered.}$

	Energy Produced per Device [MWh]					
	Winter	Spring	Summer	Autumn	Total	CF [%]
2011	259	89	120	162	628	25
2012	227	109	95	186	617	24
2013	195	110	74	188	566	22
2014	265	108	89	110	572	23
2015	279	157	92	181	707	28
2016	227	122	90	118	556	22
2017	213	110	87	241	649	26
2018	206	74	74	158	510	20
2019	221	143	82	178	622	24
2020	280	122	105	195	700	28
Mean	241	115	92	174	621	25

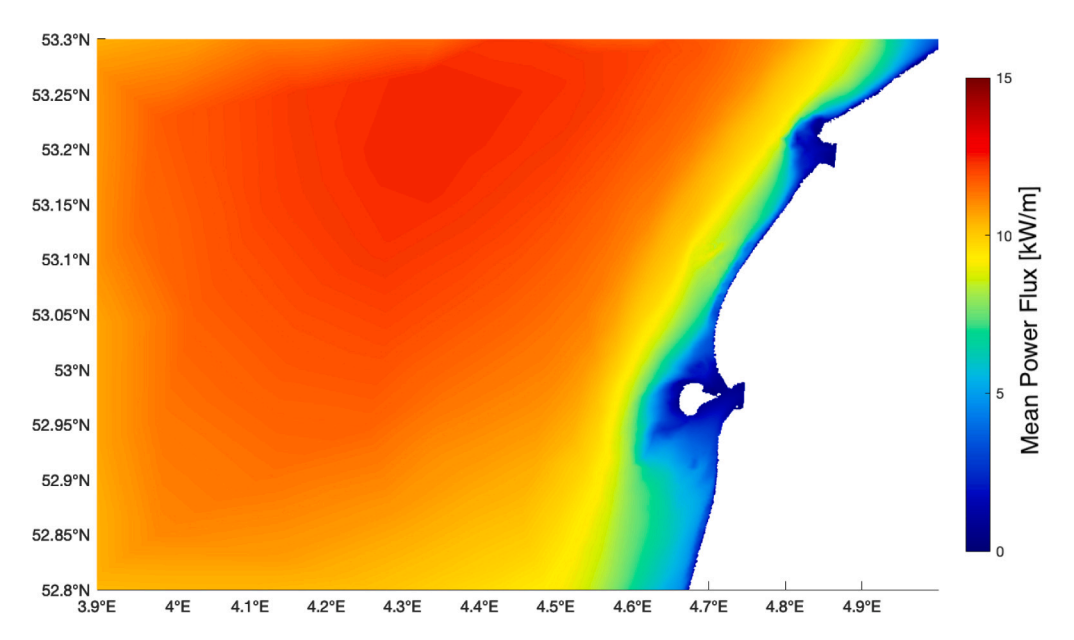


Fig. 3. Average power resource in the model domain over the 10 years spanning 2011-2020.

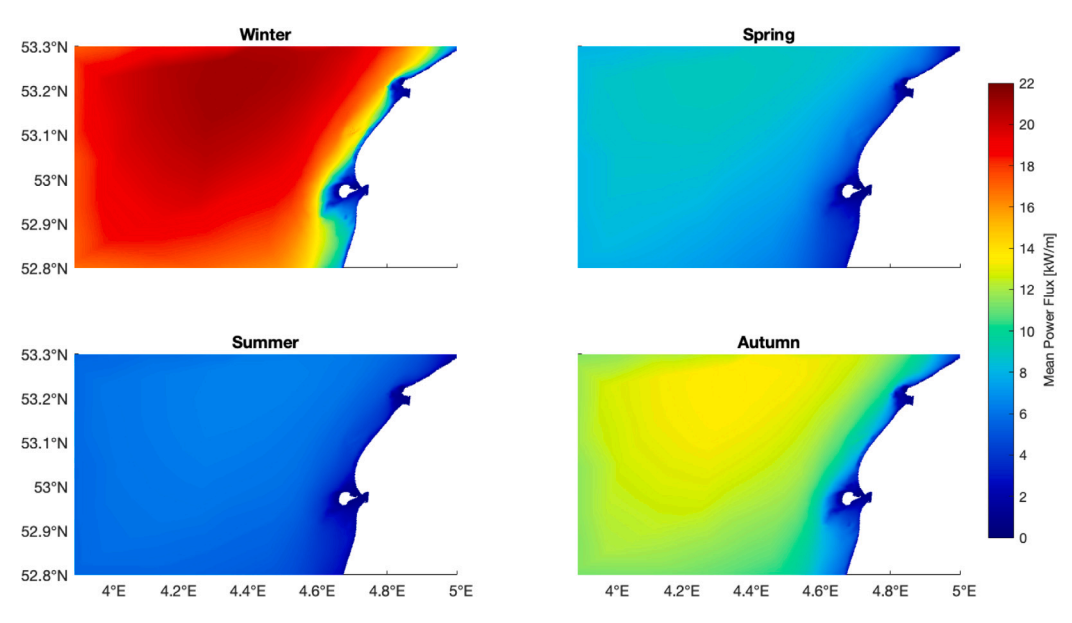


Fig. 4. Average power resource per season in the model domain over the 10 years spanning 2011-2020.

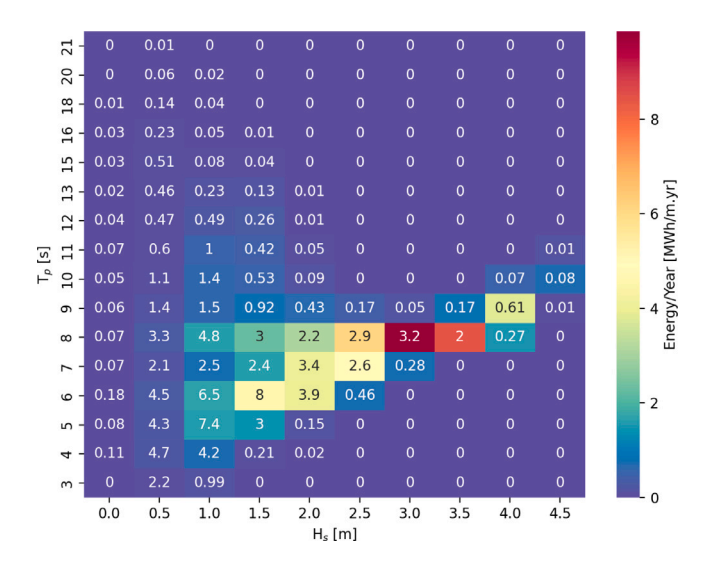


Fig. 5. Scatter diagram for the WEC site for the years 2011–2020, with a colour scale representing the average amount of annual energy flux [MWh/m·yr] associated with different sea states (parametrised by H_s and T_p). Numerical values represent mean portion of time [%] spent per year in each sea state.

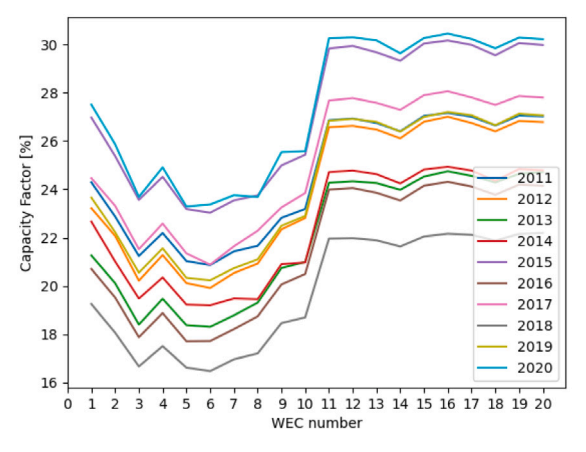
the distribution of power production over the leeward row is slightly different.

Fig. 7 showcases the discrepancy between the two methods to calculate the capacity factor, and highlights the annual variability of this quantity. From this plot, it can be seen that the capacity factor of the devices is 1–1.8% less when considering wake effects. In reality, this figure is likely to be even greater, as the methodology implemented uses wave parameters at a point immediately seaward of each device to calculate energy yield. This approach results in the reflected wave field contributing to the calculated power yield of the device, which is not consistent with reality. Despite this effect, which acts to increase the calculated yield when WECs are simulated, there is still a marked reduction compared to the baseline scenario. It is expected, therefore, that the real overestimation obtained using the traditional resource-calculation method exceeds the values demonstrated in this paper. Furthermore, it can be seen that the annual capacity factor varies by up to 8% during the 10 year period simulated.

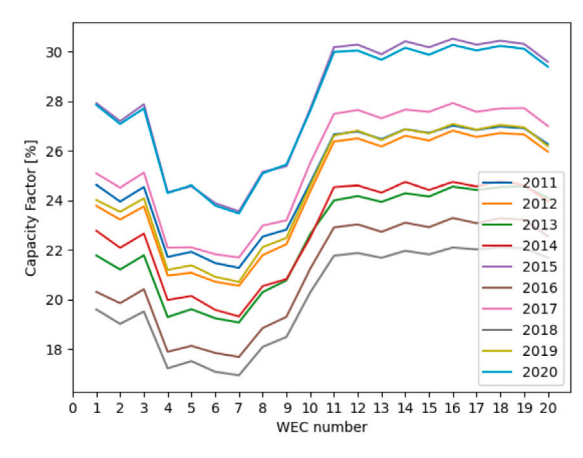
This figure also demonstrates clearly the difference in power production between the 2 array configurations considered. It can be seen that the 3L configuration has an approximately 0.5% lower average capacity factor compared to the 5L configuration, with the notable exception in 2016 in which the 5L array under-performs. From this it can be deduced not only that this wave farm is minimally sensitive to array spacing in terms of power production, but also that long-term studies are imperative to ascertain the influence of array configuration.

The dimensionless parameters associated with the WEC arrays are presented in Table 4. In particular, the q-factor associated with each configuration demonstrates the importance of considering wake effects. The q-factor represents the ratio of energy produced by an array compared to the case in which the devices are isolated. It shows that this parameter ranges from 93.2–95.7% for the 3L case, and 92.1–96.9% in the 5L case. On average, the 3L array configuration produced 5.5% less energy per year than the isolated case, and the 5L configuration produced 4.3% less.

This indicates that resource evaluations produced without considering wake effects will produce a considerable overestimation of the energy yield, and will produce a lower levelised-cost-of-energy [LCOE] than reality. For new renewable energy technologies to become financially feasible, realistic predictions must be made. The approach implemented in this work allows for realistic energy yield forecasts to be made, while also predicting the coastal impacts of the proposed farm.



(a) 3L Array Configuration.



(b) 5L Array Configuration.

Fig. 6. Capacity factor of each WEC in the array over the 10 year period between 2011–2020. WECs 1–10 are in the leeward row, and WECS 11–20 are in the seaward row.

4.3. Wake effects

Fig. 8 shows the mean reduction of the significant wave height in the 10 year period simulated, and in summer and winter conditions. From this plot the extent of the coastal region affected can be clearly observed, and the magnitude of the average nearshore impact. In summer conditions, the reduction in the wave height is small and is dissipated close to the shore. This observation can be well utilised from a public acceptance perspective, as the summer months are when the region will be most frequented by recreational users. By demonstrating that the wave field is minimally affected during this time, concerns from the public on this issue can be dissuaded. In winter, during which time the potential for power extraction is highest, the magnitude and width of the impact is greater. In the 5L configuration, the impacted region is wider, while the maximum impact in the immediate lee is less. The impact is therefore more diffuse in this case, although the power output was shown in Fig. 7 to be very similar in each case.

Fig. 9 depicts the average magnitude of the reduction in the significant wave height for different sea conditions, described by the peak period and the significant wave height. These values were calculated by taking the value for the reduction in H_s at the point at which the reduction is maximum at every timestep during the 10 years.

The values were then binned according to the T_p and H_s at the farm site, and the average value of ΔH_s for each bin was taken. Results for sea states with $H_s < 1$ m have not been shown due to the anomalies that

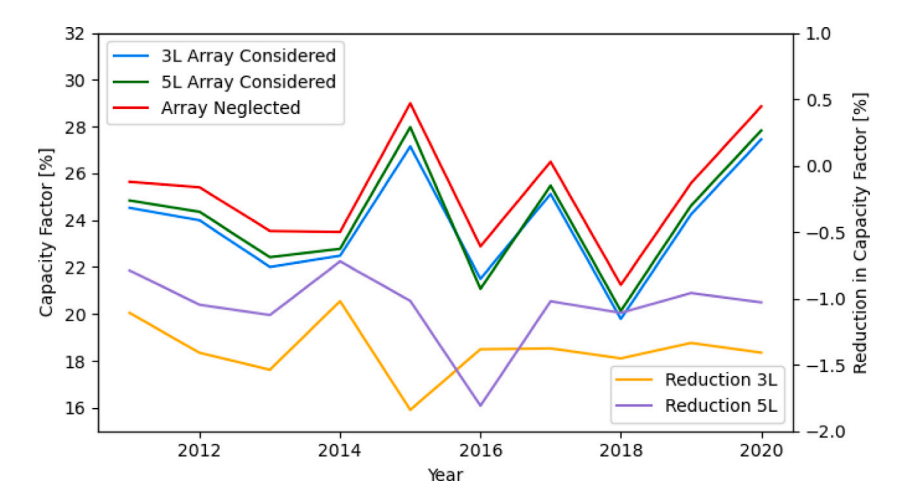


Fig. 7. Average capacity factor of the WEC farm calculated with and without wake effects considered.

Table 4
Mean capacity and q- factor of the arrays.

	Dimensionless Parameters [%]						
	Average Capacity Factor: 3L	Average Capacity Factor: 5L	Array q-factor: 3L	Array q-factor: 5L			
2011	24.5	24.8	95.7	96.9			
2012	24.0	24.4	94.4	95.9			
2013	22.0	22.4	93.5	95.2			
2014	22.5	22.8	95.7	96.9			
2015	27.1	28.0	93.7	96.5			
2016	21.5	21.1	94.0	92.1			
2017	25.1	25.5	94.8	96.1			
2018	19.8	20.1	93.2	94.8			
2019	24.2	24.6	94.8	96.3			
2020	27.4	27.8	95.1	96.4			
Mean	23.8	24.1	94.5	95.7			

may occur in this zone. It can be seen in the figure that the interaction of the wave farm with the wave field is extremely similar in each array configuration, again suggesting that the impact of the array on the coast is minimally sensitive to array spacing. It is interesting to note that the magnitude of the reduction in the wave field is dependent on both H_s and T_{-} .

It can be seen that the WEC array will most significantly affect the nearshore wave field in sea states with $T_p \sim 7.5$ –9 s, and $H_s \sim 2.25$ –3.25 m, with an average reduction of approximately 14 cm. Comparing with Fig. 5 shown in the baseline scenario, it can be seen that these sea states account for the most energy produced in this region, but are not the most frequently occurring. Conversely, the most frequently occurring sea states at the farm have $T_p \sim 4$ –8 s and $H_s \sim 0.5$ –2 m, for which the average reduction is between 0–6 cm. This suggests that although the wave farm may not have a significant effect on the nearshore wave field the majority of the time, it will reduce the effect of the sea states that are responsible for the largest amount of annual energy. It can be seen in Fig. 9 that for sea states with $H_s > 3.25$ m, the wave field is less reduced than in smaller conditions. This may be due to the nature of the interactions between the array and waves, or due to the directions from which large sea swells come from.

The configuration of the array, in which the rows run north-south, attenuates the largest amount of energy of swells approaching from the west. For an array to serve as a protective measure against storm-like conditions, particularly for OWSCs that are highly directionally dependent, it must therefore be determined from which direction this energy will come. Deciding the orientation of the farm based on this factor may, however, come at a cost to energy yield from the array. In other locations, it must also be considered that in extremely highly energetic sea states, WEC devices enter into survival mode, and cease to produce energy to prevent excessive loads on the structure, usually

by submerging/retracting the structure. In these conditions, the farm is not effective in reducing the impact of waves on the coast. In this case, however, the Oyster similar WECs go into this mode at sea states with $H_{\rm s} > 6$ m, which are not observed at this site.

A key factor that will influence longshore currents is the portion of waves that break, as broken waves create a significant amount of mass transport that must be transported back to sea via rip currents. Fig. 10 shows the mean change in the breaker index upon implementation of the WEC farm, in terms of the percentage of waves that break.

It can be seen that in both cases, the portion of waves that break at the coastline is approximately 1% less on average than in the case without a farm present. While this is a small portion of waves, a 1% reduction in the average number of broken waves over a decade may produce a cumulative morphodynamic effect that is measurable.

The way in which the breaker index is calculated in SWAN is defined in [29], calculated by determining the statistical probability of a wave exceeding the maximum possible height for an unbroken wave in the present water depth. As has been discussed previously, SWAN is unable to produce highly accurate spectral results in shallow water regions. It is therefore expected that the precise breaker index calculated by SWAN will differ from reality, however the difference between the nofarm and with-farm scenarios provides a qualitative indication that this parameter will be affected.

5. Discussion

These results highlight several key factors that should be considered when conducting a resource evaluation at a potential wave energy site. Firstly, the use of long-term data is shown to be essential as the interannual variation in the device capacity factor is as great as 8% in the

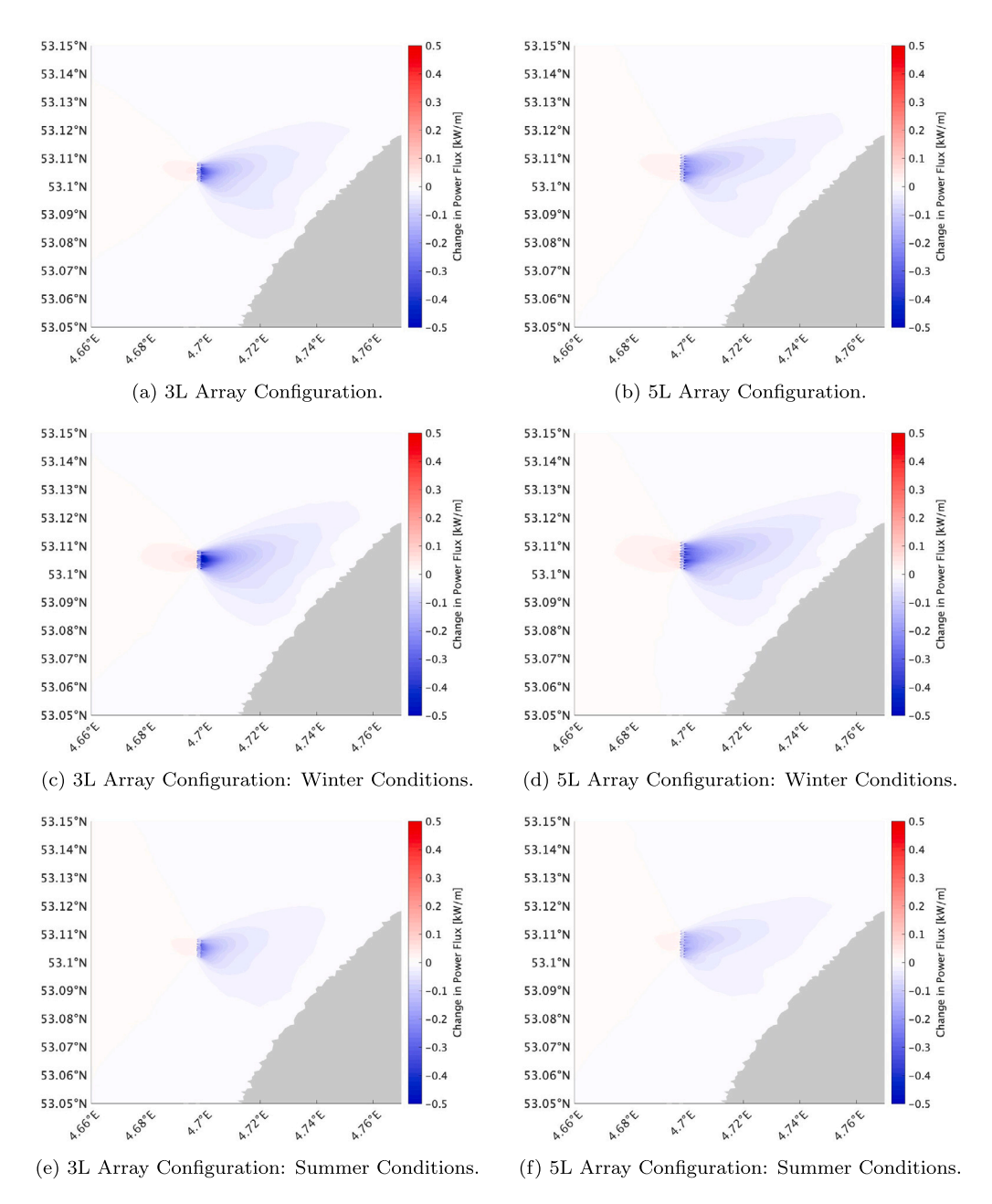


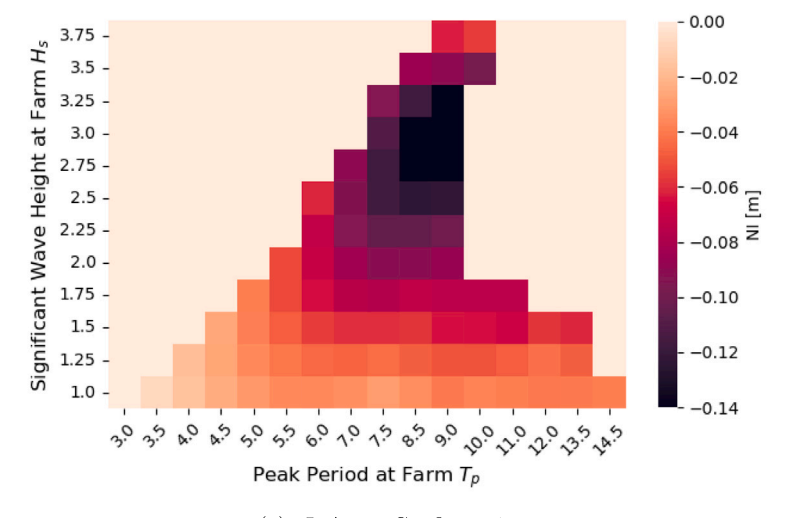
Fig. 8. Mean reduction in the significant wave height in the region surrounding the farm.

decade studied. Furthermore, the incorporation of the WEC devices into the simulations is shown to reduce the annual average of the capacity factor of the array by up to 1.8%, suggesting that the levelised-cost-of-energy of this technology will be significantly underestimated if traditional resource evaluations are used. It is expected that, in reality, the overestimation of the energy yield when wake effects are neglected is even greater than what is demonstrated by these results due to the influence of the reflected wave field on the calculated values. These reflected wave fields can be seen in Fig. 3. Despite this effect acting to raise the calculated power yield of the array, a notable reduction compared to traditional methods is still clearly shown.

The presence of the WEC arrays was shown to notably reduce the significant wave height in the region surrounding the farm. While the total average wave height at the farm site is 1.4 m, it is reduced to 1 m in the immediate lee of the 3L configuration, and 1.2 m in the 5L configuration. This effect, however, is dissipated close to the shore. In winter, the magnitude of the decrease is greater, but the

effect is still not significant at the level of the shoreline. Interestingly, the simulated results showed that the average magnitude of the reduction is both height and period dependent, however the reduction does not increase continuously with these parameters. Despite previous literature [13,30–36] suggesting that WEC arrays may provide coastal protection from high-energy events, the reduction in the wave heights was shown to be maximum at $H_s \sim 2$ –3 m, beyond which the impact reduced with increasing wave heights. Comparison of the maximum observed reductions for varying H_s demonstrated the same trend. This contradicts the proposal that WEC arrays are viable protective measures from extreme events, as it suggests that the farm will be decreasingly effective for coastal protection at wave heights even below the survival mode threshold.

To more deeply examine the potential ecological impacts of implementing WEC arrays, further analyses should be conducted. Preliminary results from the present work demonstrate that there may be changes



(a) 3L Array Configuration.

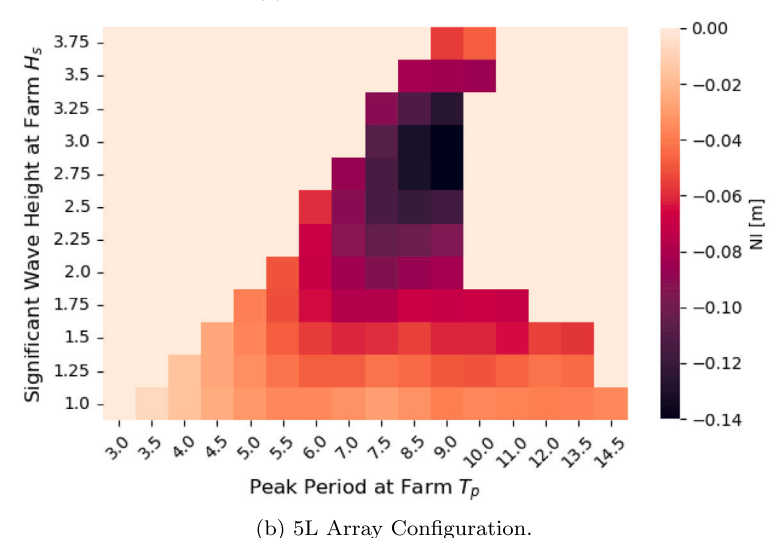


Fig. 9. Average reduction in wave height for different sea states.

to the nearshore currents as a result of the arrays, which has consequences for sediment and nutrient transport. The conducted simulations showed a reduction in the portion of breaking waves of 1%. This change indicates that currents will be affected, but are inconclusive. To more accurately assess these impacts, a coastal morphodynamic model that is more suited to simulating shallow water conditions such as XBeach should be implemented. Furthermore, the accuracy of the results could be improved in future works through the implementation of frequency and directionally dependent transmission coefficients, obtained through CFD modelling.

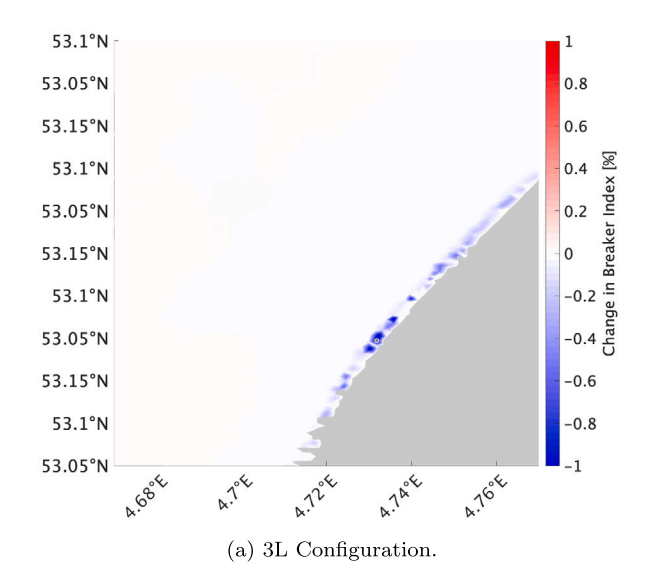
6. Conclusions

The present work has aimed to demonstrate the potential power production and the nearshore impacts on the wave climate of 20 WEC devices employed on the Dutch coast for the 10 year period spanning 2011–2020. These 2 essential stages in determining the viability of a proposed WEC farm have been streamlined into a single methodology, simulated with the spectral wave propagation model SWAN.

Analysis of the power output of the 2 array configurations demonstrated that the traditional approach for resource evaluations, in which wake effects are neglected, resulted in an overestimation of the capacity factor of between 1–1.8% for the 3L case, and 0.8–1.8% for the 5L case. In reality, it is expected that the real overestimation is higher, as the

nature of the reflective effects of the devices in SWAN also produces an overestimation compared to reality. However, the methodology considered in this work more closely represents reality compared to the traditional method. Using the revised approach, the mean capacity factor itself varied from 19.8-27.4% in the 3L case, and 20.1-28.0% in the 5L case over the 10 simulated years. The high inter-annual variability demonstrates the importance of performing long-term simulations to accurately predict the power-producing potential of an array at a particular site. The mean q-factor of the 3L array configuration was determined to be 94.5%, and the 5L configuration was 95.7%. This highlights the value of performing a resource evaluation in this way, as the determination of the LCOE for a proposed WEC project will be heavily dependent upon the predicted energy production. An overestimation of 5% on a decadal scale represents a significant amount of energy, and must be accounted for to accurately model a project.

Analysis of the impact of the WEC arrays on the significant wave height demonstrated that although there is a significant reduction in the direct lee, the effect is largely attenuated close to the shore, particularly in the summer months. As this is when recreational use is highest, this phenomenon can be helpfully utilised for public acceptance. It was shown that the impact is the greatest in conditions (H_s and T_p) responsible for the highest annual portion of energy, however it has a diminished impact in the sea states with the highest power. This



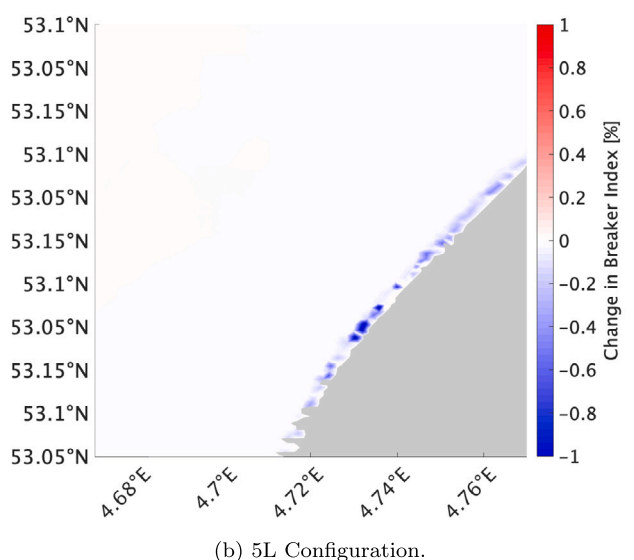


Fig. 10. Mean change in breaker index.

suggests that the use of WEC arrays as protective devices against damaging storm-like conditions may be decreasingly effective in higher energy sea states.

CRediT authorship contribution statement

Sarah Wells: Writing – original draft, Visualization, Validation, Methodology, Investigation, Formal analysis, Data curation. Matías Alday: Supervision, Methodology, Conceptualization. Jesús Maria Blanco Ilzarbe: Supervision. George Lavidas: Writing – review & editing, Writing – original draft, Supervision, Resources, Conceptualization.

Funding acknowledgements

The first author of this article was provided with scholarship from the European Union as part of the Erasmus Mundus Joint Masters Program entitled Renewable Energy in Marine Environments (REMPlus).

Declaration of competing interest

The authors declare the following financial interests/personal relationships which may be considered as potential competing interests: Sarah Wells reports financial support was provided by Erasmus Mundus Joint Master's Program REMPlus. If there are other authors, they declare that they have no known competing financial interests or personal relationships that could have appeared to influence the work reported in this paper.

Data availability

Data will be made available on request.

References

- Ritchie H, Rosado P, Roser M. Breakdown of carbon dioxide, methane and nitrous oxide emissions by sector. Our World Data 2020. https://ourworldindata.org/ emissions-by-sector.
- [2] IPCC. Climate change 2007: The physical science basis. Agenda 2007;6(07):333.
- [3] European Green Deal. Delivering the European green deal. 2024, URL https://c ommission.europa.eu/strategy-and-policy/priorities-2019-2024/european-green-deal/delivering-european-green-deal_en.
- [4] Bouckaert S, Pales AF, McGlade C, Remme U, Wanner B, Varro L, et al. Net zero by 2050: A roadmap for the global energy sector. 2021.
- [5] Commission E. Offshore renewable energy. 2024, URL https://energy.ec.europa.eu/topics/renewable-energy/offshore-renewable-energy_en.
- [6] Martinez A, Iglesias G. Wave exploitability index and wave resource classification. Renew Sustain Energy Rev 2020;134:110393.
- [7] Lavidas G, Polinder H. Wave energy in the Netherlands: Past, present and future perspectives. In: Proceedings of the 13th European wave and tidal energy conference. 2019. p. 1226.
- [8] Iglesias G, Carballo R. Wave farm impact: The role of farm-to-coast distance. Renew Energy 2014;69:375–85.
- [9] Rodriguez-Delgado C, Bergillos RJ, Ortega-Sánchez M, Iglesias G. Wave farm effects on the coast: the alongshore position. Sci Total Environ 2018;640:1176–86.
- [10] O'Dea A, Haller MC, Özkan-Haller HT. The impact of wave energy converter arrays on wave-induced forcing in the surf zone. Ocean Eng 2018. http://dx.doi. org/10.1016/J.OCEANENG.2018.03.077.
- [11] Carballo R, Iglesias G. Wave farm impact based on realistic wave-WEC interaction. Energy 2013. http://dx.doi.org/10.1016/J.ENERGY.2012.12.040.
- [12] Rodriguez-Delgado C, Bergillos RJ, Iglesias G. Dual wave farms and coastline dynamics: The role of inter-device spacing. Sci Total Environ 2019. http://dx. doi.org/10.1016/J.SCITOTENV.2018.07.110.
- [13] Berrio Y, Rivillas-Ospina G, Ruiz-Martínez G, Arango-Manrique A, Ricaurte C, Mendoza E, et al. Energy conversion and beach protection: Numerical assessment of a dual-purpose WEC farm. Renew Energy 2023. http://dx.doi.org/10.1016/J. RENENE.2023.119555.
- [14] Bento AR, Rusu E, Martinho P, Soares CG. Assessment of the changes induced by a wave energy farm in the nearshore wave conditions. Comput Geosci 2014;71:50-61.
- [15] Millar D, Smith H, Reeve D. Modelling analysis of the sensitivity of shoreline change to a wave farm. Ocean Eng 2007;34(5-6):884-901.
- [16] Lavidas G, Venugopal V. Application of numerical wave models at European coastlines: A review. Renew Sustain Energy Rev 2018;92:489–500. http://dx.doi.org/10.1016/j.rser.2018.04.112, URL https://www.sciencedirect.com/science/article/pii/S1364032118303290.
- [17] Rusu L, Onea F. Assessment of the performances of various wave energy converters along the European continental coasts. Energy 2015;82:889–904.
- [18] Majidi AG, Bingölbali B, Akpınar A. Power production performance of different wave energy converters in the Southwestern Black Sea. Int J Energy Power Eng 2020;14(7):191–5.
- [19] Guillou N, Chapalain G, Sergent P. Wave energy resource assessment for small-scale WEC near a Harbour. J Mar Sci Eng 2022;10(8):1081.
- [20] López-Ruiz A, Bergillos RJ, Raffo-Caballero JM, Ortega-Sánchez M. Towards an optimum design of wave energy converter arrays through an integrated approach of life cycle performance and operational capacity. Appl Energy 2018;209:20–32. http://dx.doi.org/10.1016/j.apenergy.2017.10.062, URL https://www.sciencedirect.com/science/article/pii/S0306261917314824.
- [21] Lavidas G, Blok K. Shifting wave energy perceptions: The case for wave energy converter (WEC) feasibility at milder resources. Renew Energy 2021:170:1143–55.
- [22] Atan R, Finnegan W, Nash S, Goggins J. The effect of arrays of wave energy converters on the nearshore wave climate. Ocean Eng 2019;172:373–84.

[23] Baki H, Gonzalez MA, Lavidas G, Alday-Gonzalez M. D6.6: Description of Ultra-High wind-wave-solar hindcast models. 2024, URL https://filelist.tudelft.nl/user_ upload/MREL_D6.6_EU-SCORES.pdf.

S. Wells et al.

- [24] Alday M, Lavidas G. The ECHOWAVE hindcast: A 30-years high resolution database for wave energy applications in north atlantic European waters. Renew Energy 2024;236:121391. http://dx.doi.org/10.1016/j.renene.2024.121391, URL https://www.sciencedirect.com/science/article/pii/S0960148124014599.
- [25] Hersbach H, Bell B, Berrisford P, Hirahara S, Horányi A, Muñoz-Sabater J, et al. The ERA5 global reanalysis. O J R Meteorol Soc 2020;146(730):1999–2049.
- [26] The SWAN team. SWAN SCIENTIFIC AND TECHNICAL DOCUMENTATION. TU Delft; 2023.
- [27] Lavidas G, Polinder H. North sea wave database (NSWD) and the need for reliable resource data: A 38 year database for metocean and wave energy assessments. Atmosphere 2019;10(9):551.
- [28] Roberts KJ, Pringle WJ. CHLNDDEV/OceanMesh2D: OceanMesh2D VX.X. 2020, http://dx.doi.org/10.5281/zenodo.1341384.
- [29] Battjes JA, Janssen J. Energy loss and set-up due to breaking of random waves. In: Coastal engineering 1978. 1978, p. 569–87.

- [30] Zanuttigh B, Angelelli E. Experimental investigation of floating wave energy converters for coastal protection purpose. Coast Eng 2013. http://dx.doi.org/ 10.1016/J.COASTALENG.2012.11.007.
- [31] Abanades J, Greaves D, Iglesias G. Coastal defence through wave farms. Coast Eng 2014. http://dx.doi.org/10.1016/J.COASTALENG.2014.06.009.
- [32] Abanades J, Greaves D, Iglesias G. Coastal defence using wave farms: The role of farm-to-coast distance. Renew Energy 2015. http://dx.doi.org/10.1016/ J.RENENE.2014.10.048.
- [33] Abanades J, Flor-Blanco G, Flor G, Iglesias G. Dual wave farms for energy production and coastal protection. 2018, http://dx.doi.org/10.1016/J.OCECOAMAN. 2018.03.038.
- [34] Bergillos RJ, López-Ruiz A, Medina-López E, Moñino A, Ortega-Sánchez M. The role of wave energy converter farms on coastal protection in eroding deltas, Guadalfeo, southern Spain. J Clean Prod 2018. http://dx.doi.org/10.1016/J. JCLEPRO.2017.10.018.
- [35] Rodriguez-Delgado C, Bergillos RJ, Iglesias G. Dual wave farms for energy production and coastal protection under sea level rise. J Clean Prod 2019. http://dx.doi.org/10.1016/J.JCLEPRO.2019.03.058.
- [36] Ozkan C, Mayo T, Passeri D. The potential of wave energy conversion to Mitigate Coastal erosion from hurricanes. J Mar Sci Eng 2022. http://dx.doi.org/10.3390/ JMSE10020143.